Forkhead Factor, FOXO3a, Induces Apoptosis of Endothelial Cells Through Activation of Matrix Metalloproteinases

Hae-Young Lee, Hyun-Jung You, Joo-Yun Won, Seock-Won Youn, Hyun-Jai Cho, Kyung-Woo Park, Woong-Yang Park, Jeong-Sun Seo, Young-Bae Park, Kenneth Walsh, Byung-Hee Oh and Hyo-Soo Kim

Arterioscler Thromb Vasc Biol 2008;28;302-308; originally published online Dec 6, 2007;
DOI: 10.1161/ATVBAHA.107.150664
Arteriosclerosis, Thrombosis, and Vascular Biology is published by the American Heart Association. 7272 Greenville Avenue, Dallas, TX 72514
 Print ISSN: 1079-5642. Online ISSN: 1524-4636

Forkhead Factor, FOXO3a, Induces Apoptosis of Endothelial Cells Through Activation of Matrix Metalloproteinases

Hae-Young Lee, Hyun-Jung You, Joo-Yun Won, Seock-Won Youn, Hyun-Jai Cho, Kyung-Woo Park, Woong-Yang Park, Jeong-Sun Seo, Young-Bae Park, Kenneth Walsh, Byung-Hee Oh, Hyo-Soo Kim

Background—The forkhead factor, FOXO3a, is known to induce apoptosis in endothelial cells (ECs). However, its effects on extracellular matrices (ECM), which are important in EC survival, remained unknown. Here, we evaluated the role of FOXO3a on EC-ECM interaction.

Methods and Results—Constitutively active FOXO3a was transduced to human umbilical vein endothelial cells by adenoviral vector (Ad-TM-FOXO3a). Ad-TM-FOXO3a transfection led to dehiscence of ECs from fibronectin-coated plates, resulting in anoikis, which was significantly reversed by matrix metalloproteinase (MMP) inhibitor, GM6001. FOXO3a increased the expression of MMP-3 (stromelysin-1) but decreased the expression of tissue inhibitors of metalloproteinases-1 (TIMP-1), which was associated with increased MMP enzymatic activity in zymography. Pathophysiologic conditions such as serum starvation or heat shock also induced activation of endogenous FOXO3a, leading to activation of MMP-3 and apoptosis, which was reversed by GM6001. Delivery of Ad-TM-FOXO3a to the intraluminal surface in vivo led to EC denudation, disrupted vascular integrity, and impaired endothelium-dependent vasorelaxation.

Conclusion—Activation of MMPs and possible ECM disruption represent novel mechanisms of FOXO3a-mediated apoptosis in ECs. **(*Arterioscler Thromb Vasc Biol*. 2008;28:302-308)**

Key Words: FOXO3a ■ MMP ■ endothelial cell ■ apoptosis

Cell-to-cell and cell-to-matrix contacts are pivotal for the maintenance of survival in anchorage-dependent cells such as endothelial cells (ECs).[1] Withdrawal of anchorage-dependent cells from their association with the ECM is known to result in anoikis, a type of apoptosis that is induced by inadequate cell-to-matrix interactions,[2,3] and proteolysis of adherens junctions disrupting endothelial monolayer integrity is known to induce apoptosis.[4,5]

The forkhead factors, which were identified as important downstream molecules of phosphoinositide-3-OH kinase (PI3K)/Akt pathway,[6,7] are known to play important roles in the regulation of apoptosis,[6,8] cell cycle arrest,[8,9] and adaptation to cellular stress.[10,11] The forkhead factors have been also reported to serve essential roles in the maintenance of vascular stability.[12] Various pathophysiologic conditions including hyperglycemia[13] have been shown to activate forkhead factors, whereas vascular protecting factors such as shear stress[14,15] and statins[16] are reported to inhibit forkhead factors in blood vessels. FOXO3a, a member of the forkhead factor family, has been reported to induce apoptosis in vascular smooth muscle cells,[6,17,18] as well as in endothelial cells.[7,19] However, the mechanism of FOXO3a-mediated apoptosis in ECs is still unclear and has not yet been fully defined.

In the present study, we identify a novel action of FOXO3a in the regulation of EC-ECM interaction. We found that the activation of FOXO3a induced detachment of endothelial cells from ECM through the activation of matrix metalloproteinase-3 (MMP-3, also called as stromelysin-1) and the suppression of tissue inhibitor of metalloproteinase-1 (TIMP-1). Here, we specify the functional significance of increased MMP activity by FOXO3a signaling in regulating EC survival and vascular integrity.

Materials and Methods

For expanded methods, please see the supplemental materials, available online at http://atvb.ahajournals.org.

Original received June 28, 2007; final version accepted November 21, 2007.

From the Innovative Research Institute for Cell Therapy (H.Y.L., H.J.Y., J.Y.W., S.W.Y., H.J.C., K.W.P., Y.B.P., H.S.K.), Seoul National University Hospital, and the Department of Internal Medicine (H.Y.L., H.J.C., K.W.P., Y.B.P., B.H.O., H.S.K.) and the Department of Biochemistry and Molecular Biology (W.-Y.P., J.-S.S.), Seoul National University College of Medicine, Seoul, Korea; and the Whitaker Cardiovascular Institute (K.W.), Boston University School of Medicine, Boston, Mass.

H.-Y.L. and H.-J.Y. contributed equally to this study.

Correspondence to Hyo-Soo Kim, MD, PhD, Department of Internal Medicine, Seoul National University College of Medicine, 28 Yongon-dong Chongno-gu Seoul 110-744 Korea. E-mail hyosoo@snu.ac.kr

Arterioscler Thromb Vasc Biol **is available at http://atvb.ahajournals.org** **DOI: 10.1161/ATVBAHA.107.150664**

Cell Culture, Adenoviral Vectors, and siRNA

Four to 6 passage human umbilical vein endothelial cells (HUVECs; Clonetics) were seeded on 2% gelatin-coated (Sigma) culture plates and incubated in endothelial growth medium (EGM bullet kit, Clonetics) with 10% fetal bovine serum.

Cell Viability and Apoptosis Assay

Viability of HUVECs was quantified using tetrazolium salt, WST-1, as instructed by the manufacturer (Roche). Apoptosis after 24 hours of adenoviral vector transfection was determined by measuring the hypodiploid fragmented DNA content using fluorescence-activated-cell sorter (FACS) analysis.[20]

Real-Time Polymerase Chain Reaction Analysis

Changes in RNA-expression of MMP-3 was determined by quantitative real-time polymerase chain reaction (PCR) as previously described.[7]

Immunoblot Analysis

Immunoblot analysis was performed by modification of the procedures described previously.[21]

Casein and Gelatin Zymography

Zymography was performed using a previously described method.[22]

Immunofluorescent Staining

For immunofluorescent staining, HUVECs were cultured on fibronectin coated dishes.

Fibronectin Degradation Assay

The degradation of fibronectin by the supernatant from Ad-TM-FOXO3a–transfected HUVEC cultured dish was evaluated.

Cell Detachment Assay

HUVECs (1×10^4 cells per well) were seeded on each well of the fibronectin (5 $\mu g/cm^2$) precoated 96-well plates and incubated at 37°C for 6 hours to allow adhesion.

In Vivo Gene Delivery in Rabbit Carotid Arteries

In vivo gene delivery was performed in carotid arteries of New Zealand White rabbits as previously described[23] to evaluate whether FOXO3a transduction induced EC denudation and functional derangement.

Histological Analysis of Endothelial Denudation

The harvested arterial segments were stained with Evans blue to identify the endothelium-denuded luminal surface.

Organ Chamber Analysis for Vascular Reactivity

Rings (4 mm long) from each carotid artery were used to assess vascular reactivity. Rings were connected to isometric force displacement transducers (Grass Instruments) and suspended in organ chambers as previously described.[23]

Statistical Analysis

All data are expressed as mean ± SD

Results

FOXO3a Induces Detachment of HUVECs from Matrix, Leading to Anoikis

HUVECs were infected by either Ad-GFP or Ad-TM-FOXO3a in the presence of serum and were harvested 24 hours thereafter. We found that Ad-TM-FOXO3a-transfected HUVECs showed significant detachment from the culture dish (Figure 1A). Survival of HUVECs was also found to decrease using a WST-1 assay (Figure 1B). Interestingly, Ad-TM-FOXO3a-transfected HUVECs were found to lose contact with plates as well as with neighboring cells at early stages after adenoviral transfection and before the appearance of other morphological changes that are associated with apoptosis (Figure 1C).

From these observations, we presumed that the activation of FOXO3a might disrupt cell-to-cell and cell-to-ECM adhesive interactions, leading to apoptosis. We also presumed that MMP activation might play a role in this process, because in microarray experiments comparing Ad-TM-FOXO3a–transfected HUVECs with Ad-GFP, the MMP-3 gene was one of the most robustly upregulated genes after FOXO3a-transduction, whereas TIMP-1 gene expression was found suppressed (data not shown).

To confirm whether MMPs play a main role in EC detachment after FOXO3a-transduction, we pretreated HUVECs with GM6001, a general MMP inhibitor, which markedly decreased EC detachment from the plate as well as from the neighboring cells (Figure 1D and 1E). Furthermore, FACS analysis for hypodiploid DNA showed about 50% reduction of apoptotic fraction in the presence of GM6001 (Figure 1F), suggesting that MMP activation might induce anoikis in FOXO3a-transduced HUVECs.

FOXO3a Induces MMP-3 in Endothelial Cells

To confirm whether the endothelial cell detachment after FOXO3a overexpression was mediated by MMP activation, we evaluated the regulation of MMP-3 after FOXO3a transduction. mRNA levels of MMP-3 was found to be significantly upregulated by real-time PCR assay. The relative fold elevation of MMP-3 transcript compared with GAPDH was 1 ± 0.3 at 16 hours, 137 ± 40 at 24 hours, and 690 ± 250 at 40 hours (Figure 2A). MMP-3 protein synthesis also increased in Ad-TM-FOXO3a–transfected HUVECs and decreased in Ad-DN-FOXO3a–transfected HUVECs. In contrast, TIMP-1 protein expression was found to be modestly decreased in Ad-TM-FOXO3a–transfected HUVECs and increased in Ad-DN-FOXO3a–transfected HUVECs. (Figure 2B).

Next, we performed casein and gelatin zymography to study whether increased MMP-3 protein retained enzymatic activity. In the casein zymography analysis, a major band corresponding to 57 kDa, and caused by the protease activity of MMP-3 was increased in media from Ad-TM-FOXO3a–transfected cells compared with media from Ad-GFP–transfected cells. In contrast, transduction of dominant-negative FOXO3a decreased MMP-3 activity in this assay (Figure 2C, upper panel). Of note, although mRNA or protein expression of MMP-2 or MMP-9 did not increase (data not shown), gelatin zymography showed an increased enzymatic activity of MMP-9 (92kDa) and MMP-2 (72kDa; Figure 2C, lower panel). Because MMP-3 is reported to activate other MMPs including MMP-2/MMP-9,[24,25] we performed MMP-3 specific knockdown experiments using MMP-3 siRNA. We found MMP-2 and MMP-9 enzymatic activity decreased with MMP-3 siRNA, suggesting that MMP-3 activation contributed to increased enzymatic activity of MMP-2 or MMP-9 after FOXO3a activation. Moreover, we also found that MMP-3 specific knockdown showed similar degree of reduction of apoptosis to that of GM6001 (supplemental Figure IIA through IID).

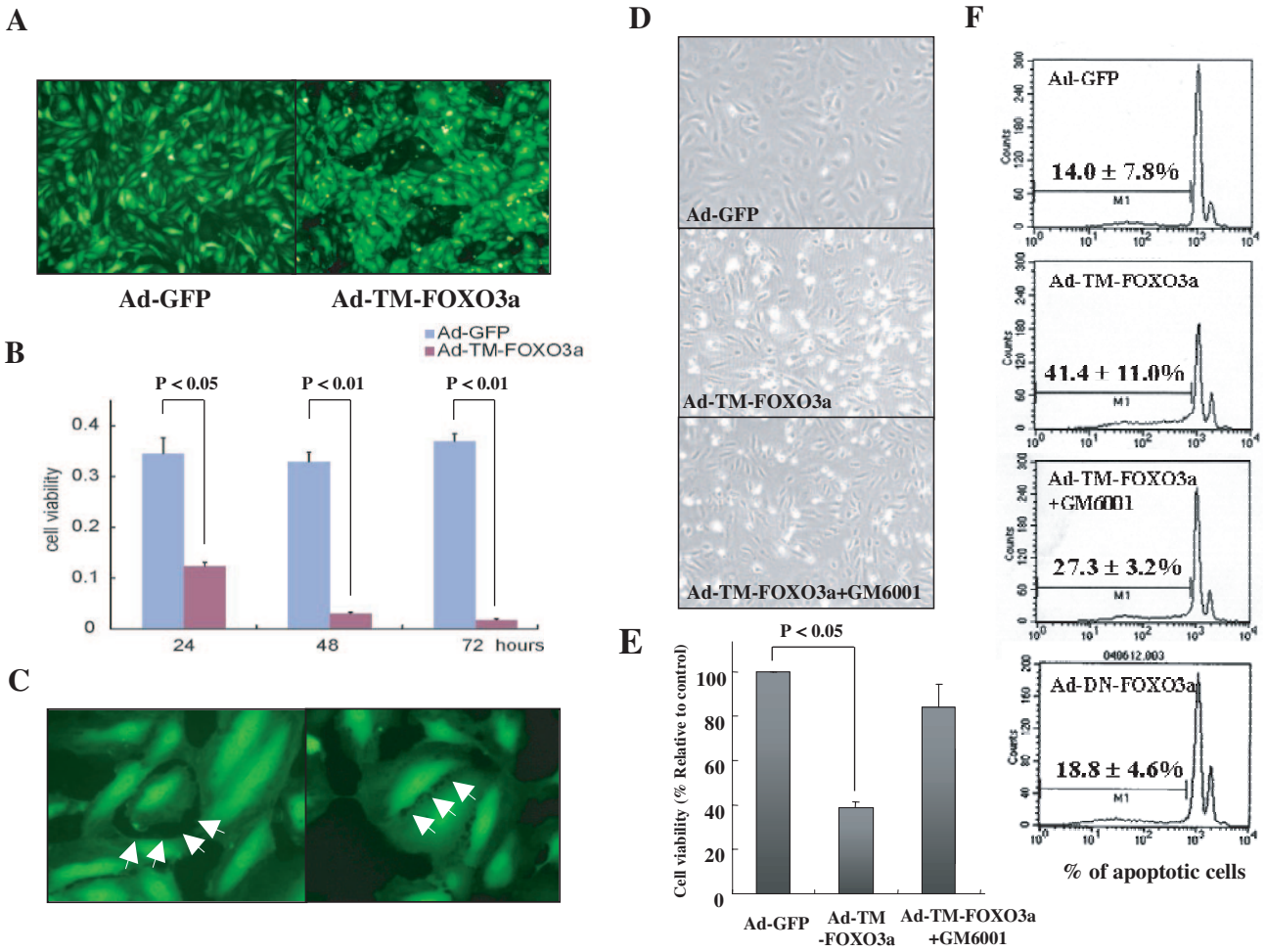

Figure 1. Effect of FOXO3a on adhesiveness and viability of HUVEC. A, Fluorescent microscopic findings of HUVECs. Magnification ×100. B, WST-1 assay of HUVEC viability. Data are expressed as mean±SE ($P<0.01$ vs Ad-GFP group, n=12). C, Fluorescent microscopic findings of HUVECs 15 hours after transfection with 25 MOI of Ad-TM-FOXO3. Magnification ×300. D, Microscopic findings of HUVECs 24 hours after transfection with Ad-GFP, Ad-TM-FOXO3, or Ad-TM-FOXO3 in the presence of GM6001. Magnification ×200. E, Quantitation of adhering cells. Data are presented as mean±SE ($P<0.05$ vs Ad-GFP–transfected group, n=16). F, FACS analysis for hypodiploid DNA. Ad-TM-FOXO3a, adenovirus of constitutively active triple-mutant FOXO3a; Ad-GFP, adenovirus of green fluorescent protein; Ad-DN-FOXO3a, adenovirus of dominant negative FOXO3a.

Stress to Endothelial Cells Induces Endogenous FOXO3a-MMP-3 Activation

To examine the role of the endogenous FOXO3a-MMP regulatory axis during the stress response, HUVECs were subjected to serum starvation or to heat shock without adenoviral transfection. An increase in active FOXO3a in nuclear fraction was detected at 6 hours after the initiation of serum starvation (supplemental Figure IIIA), which correlated with the time course of MMP activity increase in the zymography assay (supplemental Figure IIIB). In the nonstressed state, endogenous FOXO3a is located in cytoplasm and where it is inactive (supplemental Figure IIIC, left upper panel). In addition, heat shock rapidly induced intranuclear translocation and activation of endogenous FOXO3a by 30 minutes (supplemental Figure IIIC, left lower panel), which can be confirmed by the increased FOXO3a amount in nuclear fraction (supplemental Figure IIID). Enzymatic activity of MMP-3 was also found to be increased under these conditions (supplemental Figure IIIE). Heat shock induced cell death, which was significantly reduced by GM6001 treatment, suggesting that FOXO3a-MMP signaling contributes to the cytotoxicity of ECs during stress (supplemental Figure IIIF).

FOXO3a Reduces Cell-to-ECM Interaction

To investigate whether FOXO3a activation leads to ECM degradation, we evaluated the degradation of the matrix protein fibronectin after FOXO3a-transduction. After 12 hours of Ad-TM-FOXO3a transfection, fibronectin levels decreased significantly and this downregulation was effectively reversed by treatment with GM6001, suggesting that the enhanced MMP activity might contribute to the degradation of fibronectin (supplemental Figure IVA). To examine this regulation further, the supernatant from each culture dish was mixed with 5 μg of fibronectin and the degree of protein degradation was measured. The supernatant from the Ad-TM-FOXO3a–transfected culture dish displayed significantly increased fibronectin-proteolytic activity. Furthermore, the enhanced degradation was reduced by treatment with GM6001, suggesting these responses were mediated by a secreted MMP (supplemental Figures IVB and V). Next, to evaluate

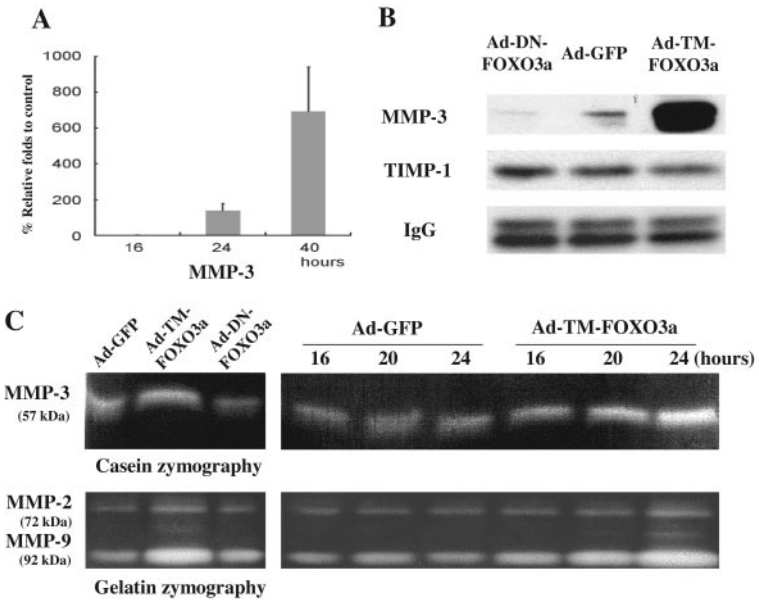

Figure 2. FOXO3a induces MMP-3 and suppresses TIMP-1. A, Quantification of real-time quantitative RT-PCR assay of MMP-3. Data are presented as mean±SE of the relative fold elevation compared with GAPDH for 3 independent experiments. B, Immunoprecipitation and immunoblot for MMP-3 and TIMP-1. C, Casein and gelatin zymography.

the functional significance of FOXO3a activation on adhesive capacity of HUVECs to ECM, we tested the adhesive capacity of HUVECs on fibronectin coated plates. FOXO3a activation significantly decreased the adhesion of HUVECs to the plates, which was reversed in the presence of GM6001 (supplemental Figure IVC).

FOXO3a Reduces Cell-to-Cell Adhesion

Next, we examined whether FOXO3a affected cell-to-cell adhesion systems maintained by the major adhesion molecules, VE-cadherin and β-catenin. Figure 3A shows uniform VE-cadherin staining over the entire cell margin, and Figure 3B shows the staining pattern of its intracellular partner β-catenin, that is present at adherens junction as well as in the cytoplasm of HUVECs (Figure 3A and 3B, left). At 24 hours after Ad-TM-FOXO3a transfection, the expression of both of these molecules was decreased at the cell-cell junctions (Figure 3A and 3B, middle). The degradation of both VE-cadherin and β-catenin was almost completely reversed in the presence GM6001, suggesting that MMP might mediate these response (Figure 3A and 3B, right). These morphological changes were corroborated by immunoblot analysis of cell lysates, which showed decreased VE-cadherin and β-catenin protein in TM-FOXO3a-transduced HUVECs and partial reversal by GM6001 (Figure 3C).

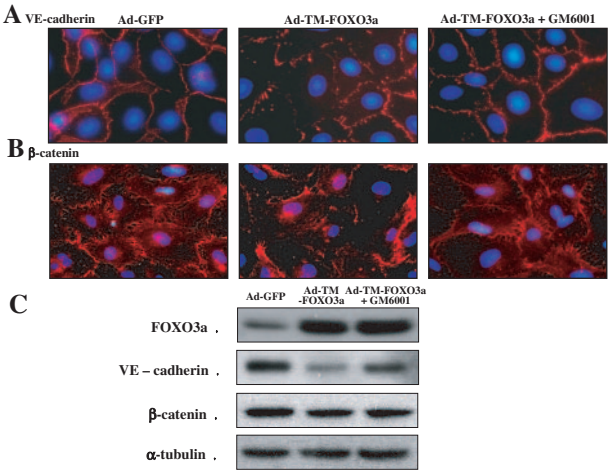

Figure 3. FOXO3a triggers cleavage of adherens junction proteins - VE-cadherin and β-catenin. A and B, Immunofluorescent microscopy of VE-cadherin (A) and β-catenin (B). HUVECs were transfected with Ad-GFP (left), Ad-TM-FOXO3a (middle), or Ad-TM-FOXO3a in the presence of GM6001 (right). Magnification ×400. C, Immunoblot analysis of VE-cadherin and β-catenin in cell lysates.

FOXO3a Activation in the Vessel Wall Induces Endothelial Denudation and Loss of Barrier Function

We evaluated vascular integrity after FOXO3a activation in rabbit carotid arteries after FOXO3a transduction. At 24 hours after Ad-TM-FOXO3a transfer, arterial segments showed significant endothelial denudation, which was markedly reversed by GM6001 (supplemental Figure VIA and VIB). Immunohistochemical staining of PECAM-1 revealed greater endothelial denudation after FOXO3a gene transfer compared with the control. Endothelial denudation was significantly reversed by GM6001, suggesting that these findings were mediated by MMPs (Figure 4A, supplemental Figure VIC). Scanning electron microscopy showed a regular and smooth-surfaced endothelial lining in the Ad-GFP group (Figure 4B, upper middle), similar to the endothelial lining of a normal, uninjured carotid artery (Figure 4B, upper left). In contrast, the luminal surface of segments harvested from the Ad-TM-FOXO3a–transfected group demonstrated an irregular endothelial lining, exposing subendothelial tissue and various stages of endothelial cells detached from the subcellular matrix (Figure 4B, lower panels). GM6001, again, significantly reversed these phenomena (Figure 4B, upper right).

FOXO3a Activation Impairs Endothelial Function

Vascular rings from each carotid artery were applied to an organ chamber system to assess both endothelium-dependent

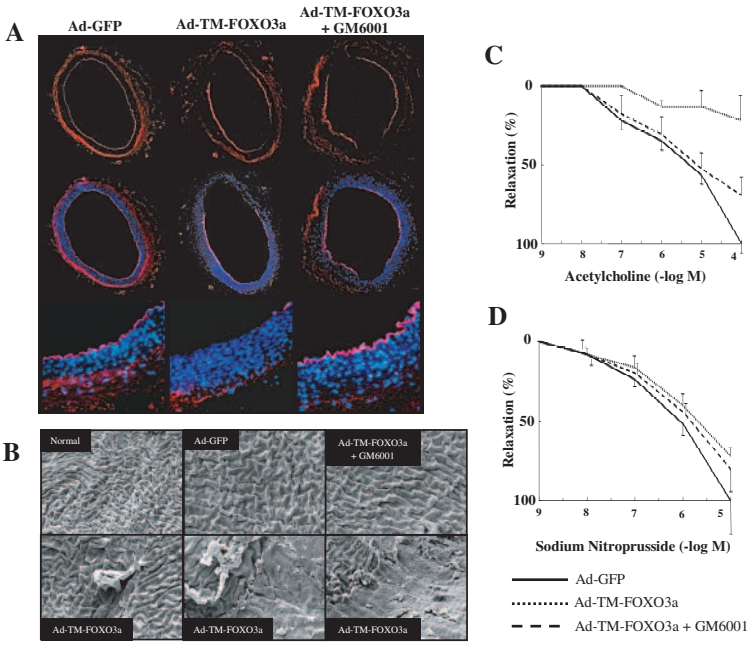

Figure 4. FOXO3a activation in vessel wall induces endothelial denudation and loss of barrier function, impairing endothelial function. A, Representative photographs of immunohistochemistry of blood vessels with PECAM-1. Upper panel, PECAM-1 staining of blood vessel; Middle panel, merged image of PECAM-1 and DAPI visualizing nuclei (Magnification ×40); Lower panel, enlargement of merged image (Magnification ×100). B, Scanning electron microscopy of luminal surface of the harvested arterial segments: normal control (upper left); treated with Ad-GFP (upper middle); Ad-TM-FOXO3a+GM6001 (upper right); Ad-TM-FOXO3a (Lower panels). Magnification ×350. C, Endothelium-dependent vasorelaxation to various concentrations of acetylcholine. D, Endothelium-independent vasodilatation to various concentrations of sodium nitroprusside. Each experiment was repeated 3 times and presented as mean±SE.

(Figure 4C) and endothelium-independent vasorelaxation (Figure 4D). Both endothelium-dependent and endothelium-independent vasorelaxation were significantly impaired in the TM-FOXO3a–transduced vessels. However, the FOXO3a-induced impairment of endothelium-dependent vasorelaxation in response to acetylcholine was much more profound compared with the relatively mild impairment of endothelium-independent vasorelaxation in response to sodium nitroprusside. In addition, the MMP blocker, GM6001, which would in theory prevent cellular detachment or anoikis, significantly reversed only the deficit in endothelium-dependent vasorelaxation (Figure 4C) and not endothelium-independent vasorelaxation (Figure 4D). These data suggest that FOXO3a activation in the vessel results in a greater impairment of endothelial-dependent vasorelaxation, and that the profound impairment of endothelium-dependent vasorelaxation may be related to anoikis.

Discussion

The most important finding of our study is that FOXO3a, a major forkhead transcription factor expressed in endothelial cells, suppressed cell-to-cell and cell-to-matrix interaction in ECs. These data suggest a novel mechanism of FOXO3a-induced apoptosis in endothelial cells. First, FOXO3a induced detachment of ECs from ECM or adjacent ECs leading to anoikis through degradation of major adherens junctional proteins such as fibronectin, VE-cadherin, and β-catenin. Second, FOXO3a induced MMP-3 and suppressed TIMP-1 expression in ECs. The finding that EC detachment, disruption of ECM and resulting anoikis were significantly reversed by GM6001, a MMP inhibitor, suggests the increased MMP activity mediates these responses. Third, these phenomena were also reproduced under pathophysiologic conditions. For example, endogenous FOXO3a induction and MMP activation were observed in ECs under stressful conditions such as serum starvation or exposure to heat shock. Finally, we showed both in vivo and ex vivo, that FOXO3a induced endothelial denudation and endothelial dysfunction in blood vessels.

FOXO3a, ECM, and EC Survival

Control of apoptosis in the endothelium is a critical issue during pathologic processes such as inflammation, vascular remodeling, and allograft vasculopathy.[26] The binding to ECM is an important survival signal to ECs. The degradation of the ECM proteins such as fibronectin has been shown to affect the apoptotic program of ECs and epithelial cells.[27–30] Another important element in EC survival is the adherens junction, in which VE-cadherin anchors the cytoskeleton of neighboring cells via β- or γ-catenin.[31–33] Both the degradation of VE-cadherin and β-catenin have been observed during apoptosis, implicating their role in apoptosis.[34,35] In the present study, we found FOXO3a activation decreased fibronectin, VE-cadherin, and β-catenin levels. This decrease could be the result of the reduced synthesis of ECM, rather than the increased degradation. In this regard, Daly et al showed that FOXO1, another forkhead transcription factor, regulated genes involving in the remodeling of ECM such as decorin, lumican, and collagen type III.[36] However, this hypothesis does not explain both the rapid decrease of ECM and adherens junction proteins after FOXO3a transduction, nor does it explain the ability of the MMP inhibitor to neutralize the effect of FOXO3a on cytotoxicity. Thus, we think that degradation by MMPs plays a major role in matrix regulation by FOXO3a.

FOXO3a and MMP3 Activation in ECs

MMPs constitute a family of extracellular proteases that are involved both in normal physiological remodeling and in pathologic degradation of the ECM.[37] ECM degradation by MMPs has been shown to be a signal that can induce apoptosis in several studies.[27,38] Moreover, exogenous

TIMP-1, the major negative regulator of MMPs, has been shown to exert a potent antiapoptotic effect on ECs.[39] Among various MMPs, we suggest MMP-3 might mediate FOXO3a-induced EC anoikis for 3 reasons. First, MMP-3 was highly upregulated in the microarray analysis of FOXO3a-induced genes, and this upregulation was confirmed at both mRNA and protein levels in the present study. Second, MMP-3 has a consensus binding site for the forkhead factors in its promoter sequences[40] suggesting transcriptional regulation by FOXO3a. Third, we found MMP-3 levels increased after FOXO3a activation. Other studies evaluating promoter sequence or microarray analysis have suggested possible regulation of some MMPs by forkhead factors,[40,41] and though PI3K/Akt pathway was suggested to increase enzymatic activity of MMPs.[42,43] However, to the best of our knowledge, this is the first report documenting a direct regulatory connection between MMPs and forkhead factors.

FOXO3a and Other MMPs Activation in ECs

Interestingly, enzymatic activities of MMP-2 and MMP-9 also increased after FOXO3a activation. However, we could not find any evidence of direct regulation of MMP-2 or MMP-9 by FOXO3a. First, neither mRNA nor the protein amount of MMP-2/MMP-9 changed after FOXO3a activation. Second, in the microarray data comparing Ad-TM-FOXO3a–transfected HUVECs with either Ad-GFP or Ad-DN-FOXO3a–transfected HUVECs, the expression pattern of MMP-2/MMP-9 did not show any significant change (data not shown). Third, the promoter sequences of MMP-2 or MMP-9 do not contain the consensus binding site for the forkhead transcription factors. Therefore, we hypothesize that the increased enzymatic activity of MMP-2 or MMP-9 observed after FOXO3a activation involves indirect regulation through changes in the expression of other molecules. We suspected that MMP-3 activation may be responsible for the activation of MMP-2/MMP-9, consistent with previous findings.[24,25] Indeed, we found that MMP-3 knockdown with siRNA led to significant reduction in the enzymatic activity of MMP-2 and MMP-9, supporting the hypothesis that MMP-3 activation contributes to increased enzymatic activity of MMP-2 or MMP-9 after FOXO3a activation. Moreover, we also found that MMP-3 knockdown revealed a significant reduction of apoptosis compared with that of GM6001, suggesting further that MMP-3 plays a key role in FOXO3a-induced ECM disruption. However, because MMP activity is also regulated by other molecules, such as TIMP-1,[25] we do not exclude the possibility that the suppression of TIMP-1 or the activation of other MMPs might result in global MMP activation. For this reason, we decided to use the general MMP inhibitor GM6001 to investigate the association between FOXO3a, MMP activity, and endothelial cell apoptosis. Finally, we cannot ascribe FOXO3a-induced apoptosis solely to MMP activation, because blocking experiment with GM6001 failed to completely reverse the effects of FOXO3a on apoptosis and anoikis. However, these findings offer new insights to the multifaceted role of FOXO3a in ECs.

In Vivo Significance of MMP Activation by FOXO3a in ECs

We found that FOXO3a activation induced endothelial denudation in vessels through in vivo gene delivery. We also found FOXO3a activation impaired both endothelium-dependent and endothelium-independent vasorelaxation through ex vivo evaluation of vasoreactivity. These effects may be caused by the proapoptotic actions of FOXO3a on ECs[7,19] as well as smooth muscle cells.[17,44,45] However, the degree of vasorelaxation impairment had a significantly greater impact on endothelium dependent function. Furthermore, GM6001 significantly reversed endothelium-dependent vasorelaxation, but had little or no effects on endothelium-independent vasorelaxation, suggesting that MMP activation may play a role in endothelial dysfunction following FOXO3a activation in vivo.

In summary, suppression of EC-ECM or EC-EC interaction represents a novel mechanism of FOXO3a-mediated EC apoptosis. Our results also suggest that MMP activation caused by deregulated FOXO3a expression could contribute to endothelial dysfunction of blood vessel.

Sources of Funding

This study was supported by the grants from the National Research Laboratory for Cardiovascular Stem Cell, Ministry of Science & Technology, and from the Innovative Research Institute for Cell Therapy (IRICT: A062260), Ministry of Health & Welfare, Republic of Korea.

Disclosures

None.

References

1. Mallat Z, Tedgui A. Apoptosis in the vasculature: mechanisms and functional importance. *Br J Pharmacol*. 2000;130:947–962.
2. Frisch SM, Francis H. Disruption of epithelial cell-matrix interactions induces apoptosis. *J Cell Biol*. 1994;124:619–626.
3. Boudreau N, Werb Z, Bissell MJ. Suppression of apoptosis by basement membrane requires three-dimensional tissue organization and withdrawal from the cell cycle. *Proc Natl Acad Sci U S A*. 1996;93:3509–3513.
4. Bannerman DD, Sathyamoorthy M, Goldblum SE. Bacterial lipopolysaccharide disrupts endothelial monolayer integrity and survival signaling events through caspase cleavage of adherens junction proteins. *J Biol Chem*. 1998;273:35371–35380.
5. Ling Y, Zhong Y, Perez-Soler R. Disruption of cell adhesion and caspase-mediated proteolysis of beta- and gamma-catenins and APC protein in paclitaxel-induced apoptosis. *Mol Pharmacol*. 2001;59:593–603.
6. Brunet A, Bonni A, Zigmond MJ, Lin MZ, Juo P, Hu LS, Anderson MJ, Arden KC, Blenis J, Greenberg ME. Akt promotes cell survival by phosphorylating and inhibiting a Forkhead transcription factor. *Cell*. 1999;96:857–868.
7. Kim HS, Skurk C, Maatz H, Shiojima I, Ivashchenko Y, Yoon SW, Park YB, Walsh K. Akt/FOXO3a signaling modulates the endothelial stress response through regulation of heat shock protein 70 expression. *Faseb J*. 2005;19:1042–1044.
8. Dijkers PF, Medema RH, Lammers JW, Koenderman L, Coffer PJ. Expression of the pro-apoptotic Bcl-2 family member Bim is regulated by the forkhead transcription factor FKHR-L1. *Curr Biol*. 2000;10:1201–1204.
9. Medema RH, Kops GJ, Bos JL, Burgering BM. AFX-like Forkhead transcription factors mediate cell-cycle regulation by Ras and PKB through p27kip1. *Nature*. 2000;404:782–787.
10. Kops GJ, Dansen TB, Polderman PE, Saarloos I, Wirtz KW, Coffer PJ, Huang TT, Bos JL, Medema RH, Burgering BM. Forkhead transcription factor FOXO3a protects quiescent cells from oxidative stress. *Nature*. 2002;419:316–321.
11. Nemoto S, Finkel T. Redox regulation of forkhead proteins through a p66shc-dependent signaling pathway. *Science*. 2002;295:2450–2452.
12. Paik JH. FOX. Os in the maintenance of vascular homoeostasis. *Biochem Soc Trans*. 2006;34:731–734.
13. Marchetti V, Menghini R, Rizza S, Vivanti A, Feccia T, Lauro D, Fukamizu A, Lauro R, Federici M. Benfotiamine counteracts glucose

toxicity effects on endothelial progenitor cell differentiation via Akt/FoxO signaling. *Diabetes*. 2006;55:2231–2237.
14. Fisslthaler B, Fleming I, Keseru B, Walsh K, Busse R. Fluid shear stress and NO decrease the activity of the hydroxy-methylglutaryl coenzyme A reductase in endothelial cells via the AMP-activated protein kinase and FoxO1. *Circ Res*. 2007;100:e12–e21.
15. Chlench S, Mecha Disassa N, Hohberg M, Hoffmann C, Pohlkamp T, Beyer G, Bongrazio M, Da Silva-Azevedo L, Baum O, Pries AR, Zakrzewicz A. Regulation of Foxo-1 and the angiopoietin-2/Tie2 system by shear stress. *FEBS Lett*. 2007;581:673–680.
16. Urbich C, Knau A, Fichtlscherer S, Walter DH, Bruhl T, Potente M, Hofmann WK, de Vos S, Zeiher AM, Dimmeler S. FOXO-dependent expression of the proapoptotic protein Bim: pivotal role for apoptosis signaling in endothelial progenitor cells. *Faseb J*. 2005;19:974–976.
17. Lee HY, Chung JW, Youn SW, Kim JY, Park KW, Koo BK, Oh BH, Park YB, Chaqour B, Walsh K, Kim HS. Forkhead transcription factor FOXO3a is a negative regulator of angiogenic immediate early gene CYR61, leading to inhibition of vascular smooth muscle cell proliferation and neointimal hyperplasia. *Circ Res*. 2007;100:372–380.
18. Suhara T, Kim HS, Kirshenbaum LA, Walsh K. Suppression of Akt signaling induces Fas ligand expression: involvement of caspase and Jun kinase activation in Akt-mediated Fas ligand regulation. *Mol Cell Biol*. 2002;22:680–691.
19. Skurk C, Maatz H, Kim HS, Yang J, Abid MR, Aird WC, Walsh K. The Akt-regulated forkhead transcription factor FOXO3a controls endothelial cell viability through modulation of the caspase-8 inhibitor FLIP. *J Biol Chem*. 2004;279:1513–1525.
20. Yang HM, Kim HS, Park KW, You HJ, Jeon SI, Youn SW, Kim SH, Oh BH, Lee MM, Park YB, Walsh K. Celecoxib, a cyclooxygenase-2 inhibitor, reduces neointimal hyperplasia through inhibition of Akt signaling. *Circulation*. 2004;110:301–308.
21. Kim HS, Skurk C, Thomas SR, Bialik A, Suhara T, Kureishi Y, Birnbaum M, Keaney JF Jr, Walsh K. Regulation of angiogenesis by glycogen synthase kinase-3beta. *J Biol Chem*. 2002;277:41888–41896.
22. Yan L, Moses MA, Huang S, Ingber DE. Adhesion-dependent control of matrix metalloproteinase-2 activation in human capillary endothelial cells. *J Cell Sci*. 2000;113(Pt 22):3979–87.
23. Kullo IJ, Mozes G, Schwartz RS, Gloviczki P, Tsutsui M, Katusic ZS, O'Brien T. Enhanced endothelium-dependent relaxations after gene transfer of recombinant endothelial nitric oxide synthase to rabbit carotid arteries. *Hypertension*. 1997;30:314–320.
24. Ogata Y, Enghild JJ, Nagase H. Matrix metalloproteinase 3 (stromelysin) activates the precursor for the human matrix metalloproteinase 9. *J Biol Chem*. 1992;267:3581–3584.
25. Nagase H. Activation mechanisms of matrix metalloproteinases. *Biol Chem*. 1997;378:151–160.
26. Karsan A, Harlan JM. Modulation of endothelial cell apoptosis: mechanisms and pathophysiological roles. *J Atheroscler Thromb*. 1996;3:75–80.
27. Boudreau N, Sympson CJ, Werb Z, Bissell MJ. Suppression of ICE and apoptosis in mammary epithelial cells by extracellular matrix. *Science*. 1995;267:891–893.
28. Kim S, Bakre M, Yin H, Varner JA. Inhibition of endothelial cell survival and angiogenesis by protein kinase A. *J Clin Invest*. 2002;110:933–941.
29. Werb Z. ECM and cell surface proteolysis: regulating cellular ecology. *Cell*. 1997;91:439–442.
30. Diaz C, Valverde L, Brenes O, Rucavado A, Gutierrez JM. Characterization of events associated with apoptosis/anoikis induced by snake venom metalloproteinase BaP1 on human endothelial cells. *J Cell Biochem*. 2005;94:520–528.
31. Lampugnani MG, Corada M, Caveda L, Breviario F, Ayalon O, Geiger B, Dejana E. The molecular organization of endothelial cell to cell junctions: differential association of plakoglobin, beta-catenin, and alpha-catenin with vascular endothelial cadherin (VE-cadherin). *J Cell Biol*. 1995;129:203–217.
32. Dejana E, Spagnuolo R, Bazzoni G. Interendothelial junctions and their role in the control of angiogenesis, vascular permeability and leukocyte transmigration. *Thromb Haemost*. 2001;86:308–315.
33. Ivanov DB, Philippova MP, Tkachuk VA. Structure and functions of classical cadherins. *Biochemistry (Mosc)*. 2001;66:1174–1186.
34. Herren B, Levkau B, Raines EW, Ross R. Cleavage of beta-catenin and plakoglobin and shedding of VE-cadherin during endothelial apoptosis: evidence for a role for caspases and metalloproteinases. *Mol Biol Cell*. 1998;9:1589–1601.
35. Steinhusen U, Weiske J, Badock V, Tauber R, Bommert K, Huber O. Cleavage and shedding of E-cadherin after induction of apoptosis. *J Biol Chem*. 2001;276:4972–4980.
36. Daly C, Wong V, Burova E, Wei Y, Zabski S, Griffiths J, Lai KM, Lin HC, Ioffe E, Yancopoulos GD, Rudge JS. Angiopoietin-1 modulates endothelial cell function and gene expression via the transcription factor FKHR (FOXO1). *Genes Dev*. 2004;18:1060–1071.
37. Imai K, Hiramatsu A, Fukushima D, Pierschbacher MD, Okada Y. Degradation of decorin by matrix metalloproteinases: identification of the cleavage sites, kinetic analyses and transforming growth factor-beta1 release. *Biochem J*. 1997;322(Pt 3):809–14.
38. Wu WB, Chang SC, Liau MY, Huang TF. Purification, molecular cloning and mechanism of action of graminelysin I, a snake-venom-derived metalloproteinase that induces apoptosis of human endothelial cells. *Biochem J*. 2001;357:719–728.
39. Boulday G, Fitau J, Coupel S, Soulillou JP, Charreau B. Exogenous tissue inhibitor of metalloproteinase-1 promotes endothelial cell survival through activation of the phosphatidylinositol 3-kinase/akt pathway. *Ann N Y Acad Sci*. 2004;1030:28–36.
40. Samatar AA, Wang L, Mirza A, Koseoglu S, Liu S, Kumar CC. Transforming growth factor-beta 2 is a transcriptional target for Akt/protein kinase B via forkhead transcription factor. *J Biol Chem*. 2002;277:28118–28126.
41. Potente M, Urbich C, Sasaki K, Hofmann WK, Heeschen C, Aicher A, Kollipara R, DePinho RA, Zeiher AM, Dimmeler S. Involvement of Foxo transcription factors in angiogenesis and postnatal neovascularization. *J Clin Invest*. 2005;115:2382–2392.
42. Bae IH, Park MJ, Yoon SH, Kang SW, Lee SS, Choi KM, Um HD. Bcl-w promotes gastric cancer cell invasion by inducing matrix metalloproteinase-2 expression via phosphoinositide 3-kinase, Akt, and Sp1. *Cancer Res*. 2006;66:4991–4995.
43. Wang L, Zhang ZG, Zhang RL, Gregg SR, Hozeska-Solgot A, LeTourneau Y, Wang Y, Chopp M. Matrix metalloproteinase 2 (MMP2) and MMP9 secreted by erythropoietin-activated endothelial cells promote neural progenitor cell migration. *J Neurosci*. 2006;26:5996–6003.
44. Park KW, Kim DH, You HJ, Sir JJ, Jeon SI, Youn SW, Yang HM, Skurk C, Park YB, Walsh K, Kim HS. Activated forkhead transcription factor inhibits neointimal hyperplasia after angioplasty through induction of p27. *Arterioscler Thromb Vasc Biol*. 2005;25:742–747.
45. Abid MR, Yano K, Guo S, Patel VI, Shrikhande G, Spokes KC, Ferran C, Aird WC. Forkhead transcription factors inhibit vascular smooth muscle cell proliferation and neointimal hyperplasia. *J Biol Chem*. 2005;280:29864–29873.

Materials and methods

Cell culture, adenoviral vectors, and siRNA

Four to six passage human umbilical vein endothelial cells (HUVEC, Clonetics™) were seeded on 2% gelatin-coated (Sigma, St. Louis, MO) culture plates and incubated in endothelial growth medium (EGM bullet kit, Clonetics) with 10% fetal bovine serum.

To evaluate the role of FOXO3a, an adenoviral vector expressing constitutively-active triple-mutant FOXO3a (Ad-TM-FOXO3a) was used as previously described[1,2]. Briefly, Ad-TM-FOXO3a was constructed by replacing three phosphorylation sites, Thr32, Ser253, and Ser315 with alanine residues, thus unphosphorylatable by Akt. And to analyze the intracellular localization or behavior of FOXO3a, we used an adenoviral vector expressing wild type form (Ad-WT-FOXO3a), which was also tagged with hemagglutinin sequence. For blocking experiment, an adenoviral vector expressing dominant-negative form (Ad-DN-FOXO3a), of which transactivation domain from the C terminus was deleted, was used. As a control, an adenoviral vector expressing green fluorescence protein (Ad-GFP) was used.

For gene transduction, cells were transfected with 25MOI of the adenoviral vector. With this dose, we confirmed the transfection efficacy was more than 90% at 24 hours.

As each adenoviral vector also contained GFP sequence, transfection efficacy can be confirmed by visualization of the green fluorescence (GFP) of transduced cell (Figure 1A). And we presented the baseline validation data regarding adenoviral vector in the supplemental figure 1.

For specific blockage of MMP-3, MMP-3 Stealth™ RNAi (or siRNA) with oligofectamine™ reagents as were used following manufacturer's instructions (Invitrogen). A control siRNA was also purchased from Invitrogen. Control siRNA or MMP-3 siRNA were treated 24 hours prior to the indicated adenovirus instillation.

Cell viability and apoptosis assay

Subconfluent HUVECs in 96-well plates were infected with adenoviral vectors and cell viability was quantified using tetrazolium salt, WST-1, as instructed by the manufacturer (Roche). Apoptosis after 24 hours of adenoviral vector transfection was determined by measuring the hypodiploid, fragmented, DNA content using FACS analysis[3]. For blocking experiment, we treated HUVECs with 10μM GM6001 (Chemicon), an MMP inhibitor, for 18 hours from 6 hours post infection.

Real-time PCR analysis

Changes in RNA-expression of MMP-3 was determined by quantitative real-time PCR as previously described[4]. Primers and probes used were as follows: forward primer: 5`-TCT CGT TGC TGC TCA TGA AAT T-3`; reverse primer: 5`-TAG AGT GGG TAC ATC AAA GCT TCA G-3`; probe: 5`-6FAM-CTC CCT GGG TCT CTT TCA CTC AGC CA-TAMRA-3. Fold changes in gene expression were determined using the Ct method. To standardize the quantification of the genes, GAPDH from each sample was quantified and the selected genes were normalized to GAPDH.

Immunoblot analysis

Immunoblot analysis was performed by modification of the procedures described previously[5]. Primary antibodies used in this study are as follows: anti-FOXO3a (rabbit polyclonal IgG, Upstate Biotechnology, 1:1000), anti-MMP-3 (R&D systems) 1:500, anti-fibronectin 1:500 (BD transduction laboratories), anti-β-catenin 1:500 (BD transduction laboratories) and anti-VE-cadherin 1:500 (BD transduction laboratories). For immunoblot of MMP-3 and TIMP-1, immunoprecipitation was performed for protein concentration.

Casein and gelatin zymography

Zymography was performed using a previously described method[6]. Briefly, samples of media conditioned by cell culture under different experimental conditions were separated on an 8% polyacrylamide gel containing 0.1% casein or gelatin. After electrophoresis, gels were stained with 0.05% Coomassie Brilliant Blue R250 (Sigma Co.) and the location of caseinolytic and gelationlytic activity detected as clear bands.

Immunofluorescent staining

For immunofluorescent staining, HUVECs were cultured on fibronectin coated dishes. After 12 hour of adenoviral transfection, HUVECs were fixed with 100% methanol for 30 minutes at -20℃, and blocked by incubation with 1% BSA in PBS for 30 minutes at room temperature. Cells were then reacted with either mouse monoclonal antibody against fibronectin (1:50 dilution), β-catenin (1:100 dilution), or VE-cadherin (1:100 dilution) overnight at 4℃. Cells were incubated for 1 hour with PE-conjugated goat anti-mouse IgG antibody at a 1:50 dilution and then, with 4,6-diamidino-2-phenylindole(DAPI) for 20 minutes to visualize nuclei.

Fibronectin degradation assay.

The degradation of fibronectin by the supernatant from Ad-TM-FOXO3a transfected

HUVEC cultured dish was evaluated. Supernatant from each culture plate was mixed with 5μg of fibronectin and incubated at 37℃ for 24 hours. The reaction was terminated by the addition of EDTA and the proteins were electrophoresed by 8% SDS-PAGE gel under reducing condition. The transferred SDS-PAGE gel was stained with Coomassie Brilliant Blue and the degree of digestion was evaluated by densitometry.

Cell detachment assay

HUVECs ($1x10^4$cells/well) were seeded on each well of the fibronectin ($5\mu g/cm^2$) precoated 96 well plates and incubated at 37℃ for 6 hours to allow adhesion. After cell adhesion, 25 MOI of adenoviral vectors were added to each conditioned well. After incubation for 24 hours, detached cells were removed by two washes with PBS. Residual viable cells were quantified by the WST-1 assay.

In vivo gene delivery in rabbit carotid arteries

All animal experiments were performed after receiving approval of the Institutional Animal Care and Use Committee (IACUC) of Clinical Research Institute in Seoul National University Hospital (AAALAC accredited facility). And National Research Council (NRC) guidelines for the care and use of laboratory animals were observed

(revised 1996). In vivo gene delivery was performed in carotid arteries of New Zealand White rabbits as previously described[7] to evaluate whether FOXO3a transduction induced EC denudation and functional derangement. Briefly, animals were given an intramuscular injection of ketamine (1.2mg/kg) and xylazine (0.3mg/kg) for sedation and anesthesia. Paramedian cervical incisions were made in the anterior neck, and the common carotid arteries were exposed bilaterally by blunt dissection. Branches of the carotid artery were tied off using 5-0 ethilon sutures. After the administration of heparin (100 U/kg), proximal and distal vascular clamps were applied to the carotid artery, and a 24-gauge angiocatheter was inserted into the distal part of the isolated segment. The needle was withdrawn and blood removed from the segment of the artery using a gauze wick at the open end of the angiocatheter. A mixture containing the each adenoviral vector (final concentration: 3.5×10^9 pfu/400μL) was then instilled intraluminally via the catheter. After 30 minutes, vascular clamps were removed, and flow was restored. In case of the blocking experiments, 0.5M of GM6001 was instilled simultaneously. Six hours later, the animals were euthanized and carotid arteries were isolated and harvested.

Histologic analysis of endothelial denudation

The harvested arterial segments were stained with Evans blue to identify the

endothelium-denuded luminal surface. The endothelium-retained area was defined macroscopically as the area that was not stained with the Evans blue dye. Another portion of the harvested vessels were used for immunohistochemistry, performed as previously described[8,9]. The primary antibody used was anti-rabbit CD31 PECAM-1 monoclonal antibody (1:200 dilution; Transduction laboratories). Each arterial specimen was blindly analyzed by computerized morphometry using Image Pro Plus Analyzer Version 4.5 (Media Cybernetics). Endothelial coverage was assessed by the percentage of PECAM-1 positive circumference versus total in three different sections. The extent of EC detachment was analyzed using scanning electron microscopy with standard techniques[10].

Organ chamber analysis for vascular reactivity

Rings (4 mm long) from each carotid artery were used to assess vascular reactivity. Rings were connected to isometric force displacement transducers (Grass Instruments) and suspended in organ chambers as previously described[7]. Using acetylcholine and sodium nitroprusside, endothelium-dependent and endothelium-independent relaxation was evaluated using standard methods[11].

Statistical analysis

All data are expressed as mean ± SD. A 2-tailed *t*-test was used to compare continuous variables. The comparisons of means from in vitro studies were performed using the Mann-Whitney U test due to small sample numbers. All calculations were performed using SPSS 13.0, and $p < 0.05$ was considered statistically significant.

References for methods

1. He TC, Zhou S, da Costa LT, Yu J, Kinzler KW, Vogelstein B. A simplified system for generating recombinant adenoviruses. *Proc Natl Acad Sci U S A*. 1998;95:2509-14.
2. Skurk C, Maatz H, Kim HS, Yang J, Abid MR, Aird WC, Walsh K. The Akt-regulated forkhead transcription factor FOXO3a controls endothelial cell viability through modulation of the caspase-8 inhibitor FLIP. *J Biol Chem*. 2004;279:1513-25.
3. Yang HM, Kim HS, Park KW, You HJ, Jeon SI, Youn SW, Kim SH, Oh BH, Lee MM, Park YB, Walsh K. Celecoxib, a cyclooxygenase-2 inhibitor, reduces neointimal hyperplasia through inhibition of Akt signaling. *Circulation*. 2004;110:301-8.
4. Kim HS, Skurk C, Maatz H, Shiojima I, Ivashchenko Y, Yoon SW, Park YB, Walsh K. Akt/FOXO3a signaling modulates the endothelial stress response through regulation of heat shock protein 70 expression. *Faseb J*. 2005;19:1042-4.
5. Kim HS, Skurk C, Thomas SR, Bialik A, Suhara T, Kureishi Y, Birnbaum M, Keaney JF, Jr., Walsh K. Regulation of angiogenesis by glycogen synthase kinase-3beta. *J Biol Chem*. 2002;277:41888-96.
6. Yan L, Moses MA, Huang S, Ingber DE. Adhesion-dependent control of matrix metalloproteinase-2 activation in human capillary endothelial cells. *J Cell Sci*.

2000;113 (Pt 22):3979-87.

7. Kullo IJ, Mozes G, Schwartz RS, Gloviczki P, Tsutsui M, Katusic ZS, O'Brien T. Enhanced endothelium-dependent relaxations after gene transfer of recombinant endothelial nitric oxide synthase to rabbit carotid arteries. *Hypertension*. 1997;30:314-20.
8. Park KW, Yang HM, Youn SW, Yang HJ, Chae IH, Oh BH, Lee MM, Park YB, Choi YS, Kim HS, Walsh K. Constitutively active glycogen synthase kinase-3beta gene transfer sustains apoptosis, inhibits proliferation of vascular smooth muscle cells, and reduces neointima formation after balloon injury in rats. *Arteriosclerosis, Thrombosis & Vascular Biology*. 2003;23:1364-9.
9. Park KW, Kim DH, You HJ, Sir JJ, Jeon SI, Youn SW, Yang HM, Skurk C, Park YB, Walsh K, Kim HS. Activated forkhead transcription factor inhibits neointimal hyperplasia after angioplasty through induction of p27. *Arterioscler Thromb Vasc Biol*. 2005;25:742-7.
10. Waksman R, Robinson KA, Crocker IR, Wang C, Gravanis MB, Cipolla GD, Hillstead RA, King SB, 3rd. Intracoronary low-dose beta-irradiation inhibits neointima formation after coronary artery balloon injury in the swine restenosis model. *Circulation*. 1995;92:3025-31.
11. Gonzales RJ, Carter RW, Kanagy NL. Laboratory demonstration of vascular smooth muscle function using rat aortic ring segments. *Adv Physiol Educ*. 2000;24:13-21.

Supplemental figure 1. Validation of adenoviral vectors

A. Confirmation of unphosphorylatable FOXO3a

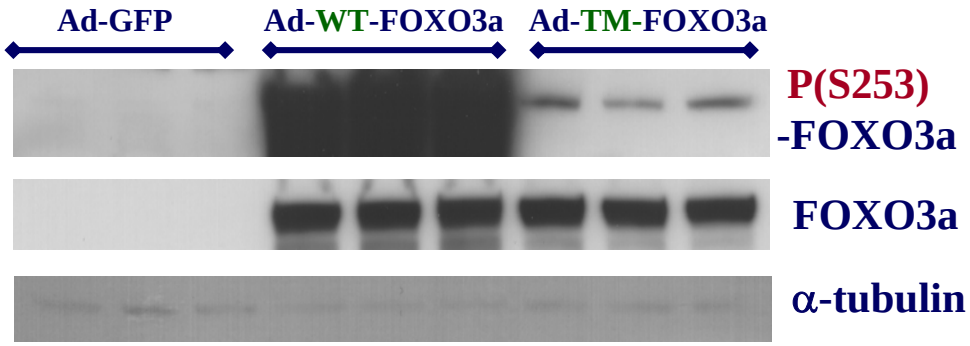

Subconfluent HUVEC were infected with adenovirus at 25MOI each for 20 hours in EGM2%.

B. Confirmation of WT-, TM-, DN-FOXO3a

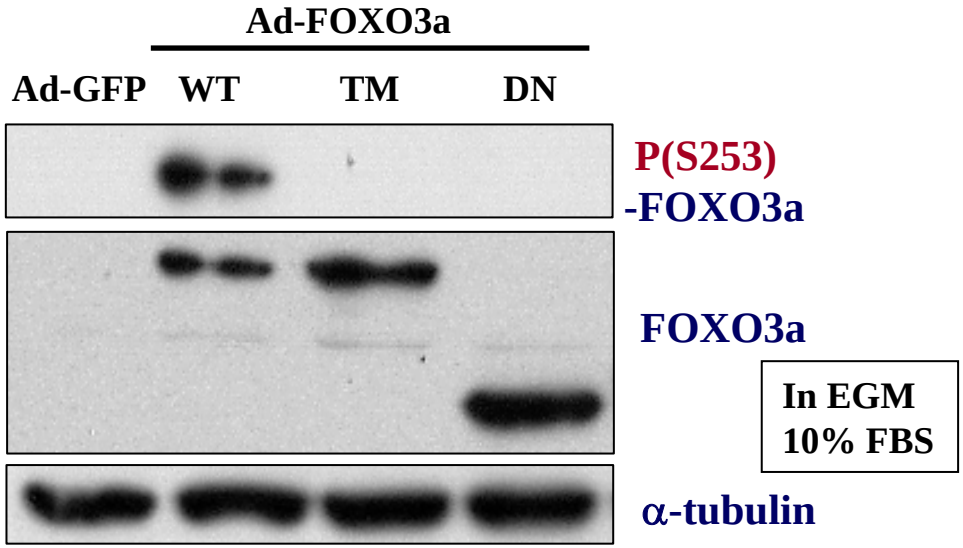

C. Evaluation of cytotoxicity

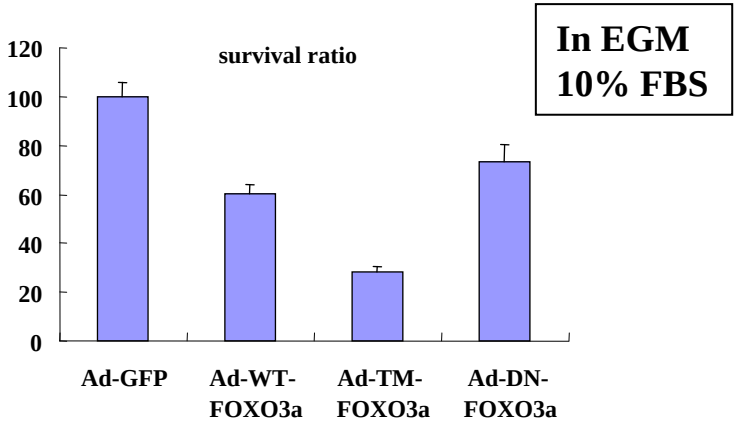

D. FACS analysis evaluating apoptotic fraction

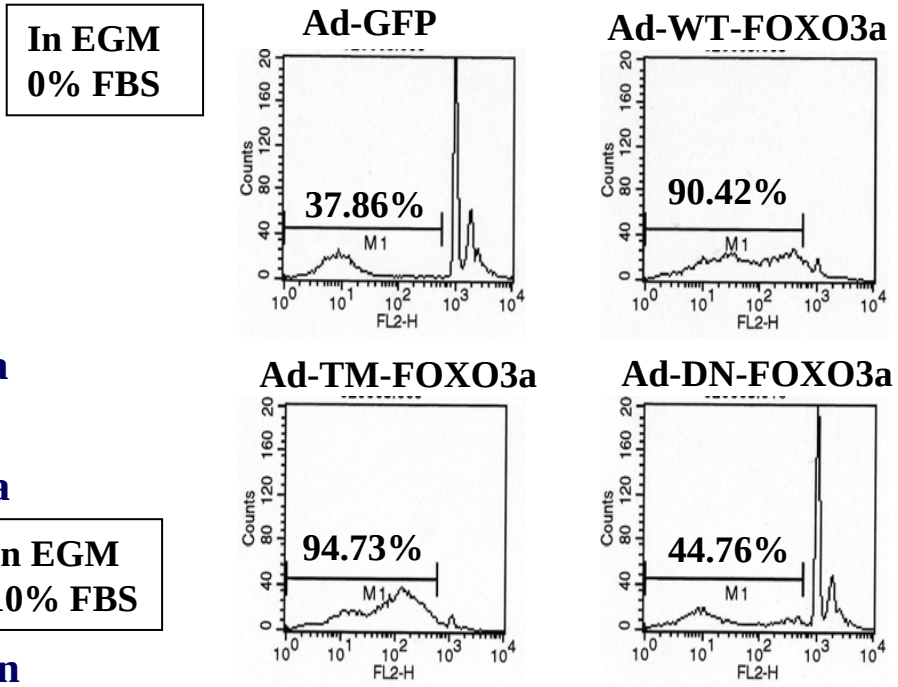

Supplemental figure 2. MMP-3 knock-down experiments using MMP-3 siRNA

A. RT-PCR validating MMP-3 knock-down

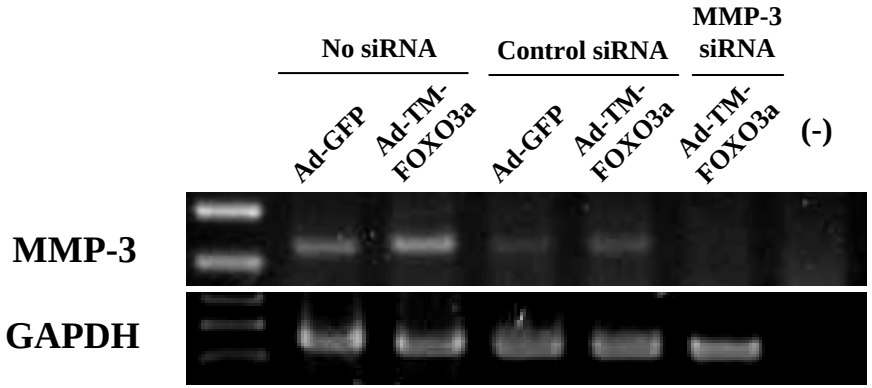

B. Casein and gelatin zymography

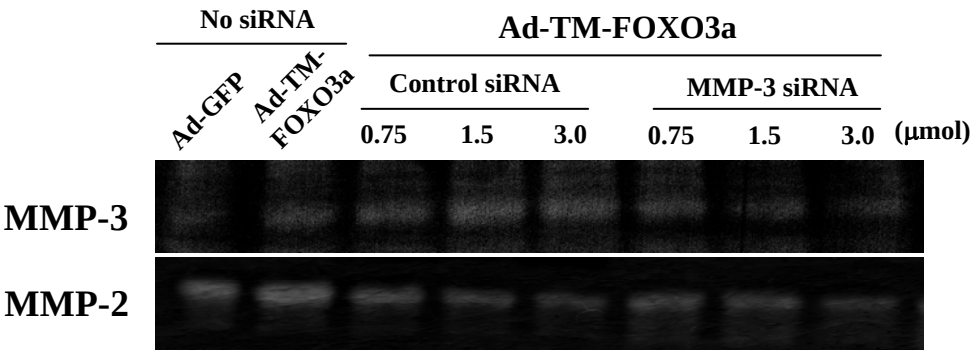

C. Morphologic change of HUVECs 16 hours after transfection of the indicated adenovirus ± siRNA.

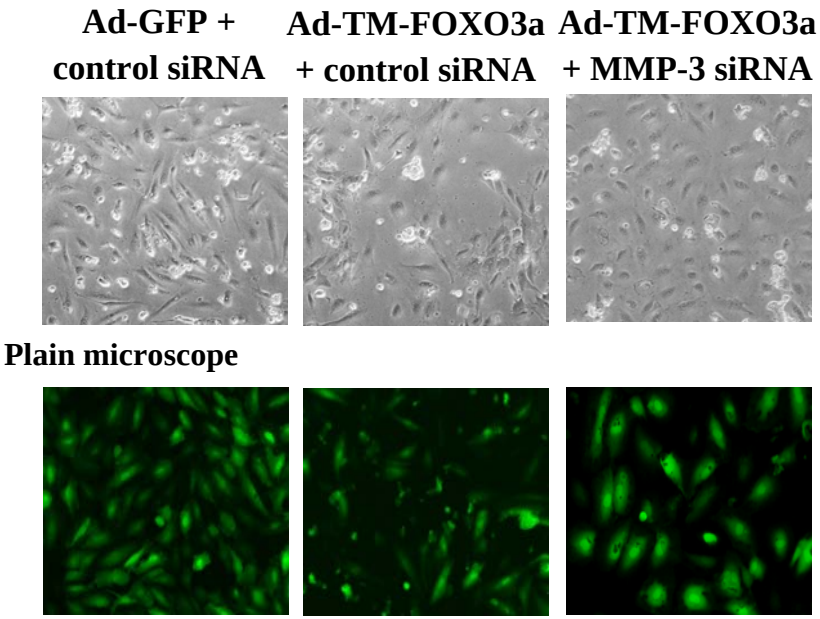

D. FACS analysis evaluating apoptotic fraction 16 hours after transfection of the indicated adenovirus ± siRNA.

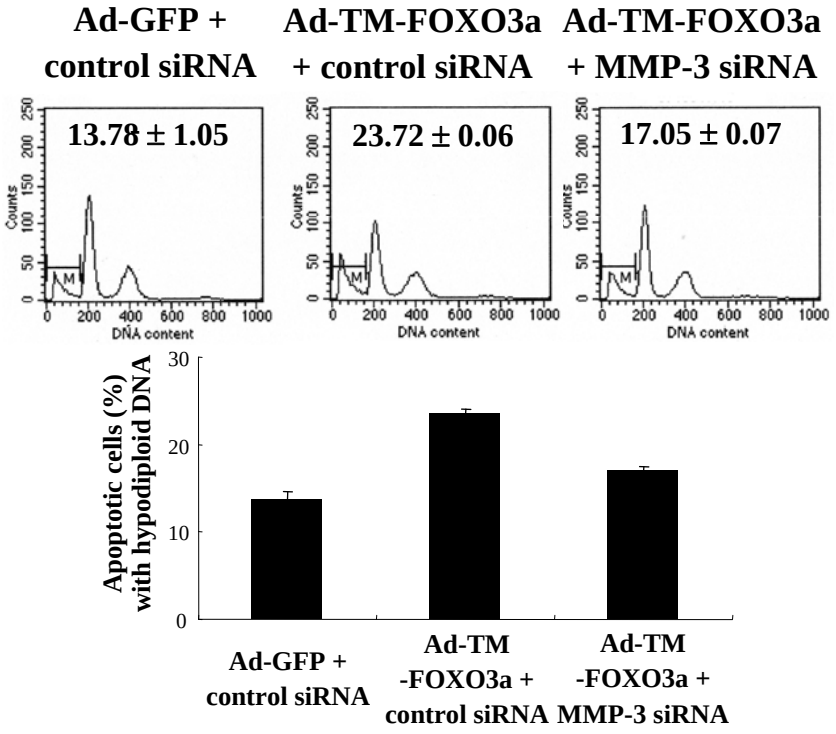

Supplemental figure 3. Endogenous FOXO3a-MMP activation under stressful conditions.

A. Serial immunoblot of endogenous FOXO3a after serum starvation

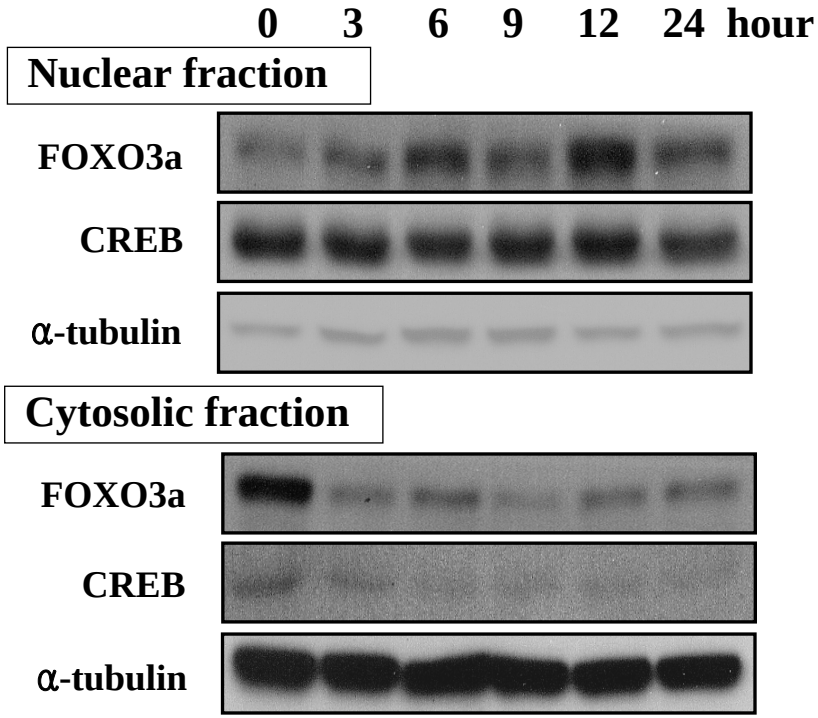

B. Casein and gelatin zymography

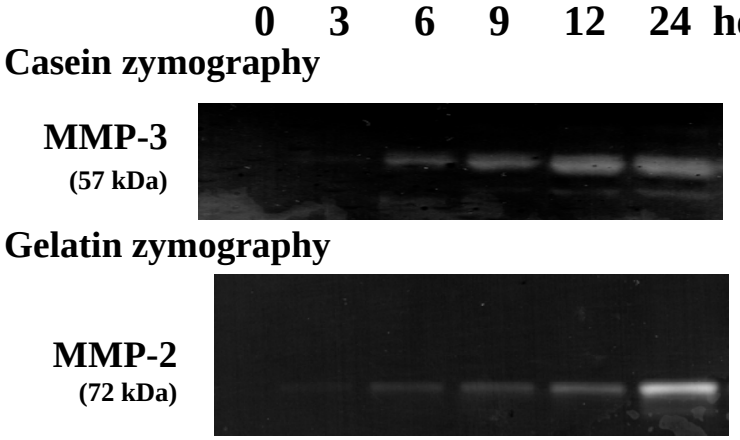

C. Immunofluorescent staining for endogenous FOXO3a after heat incubation (42°C)

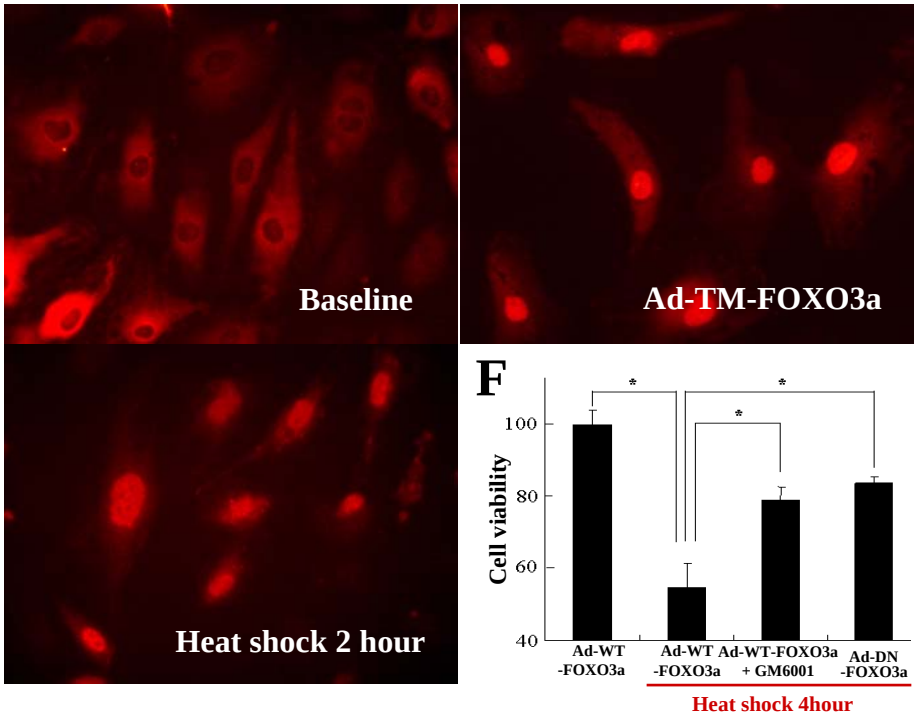

D. Immunoblot FOXO3a after heat shock.

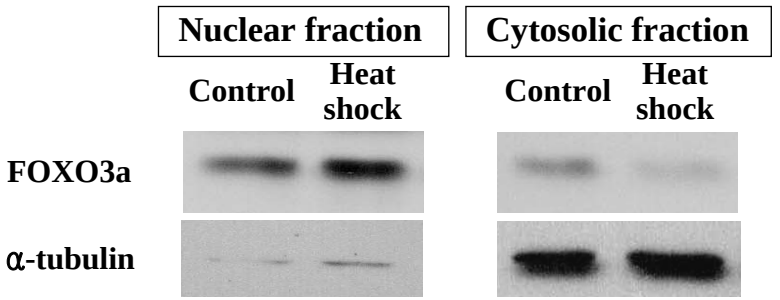

E. Casein zymography for MMP3

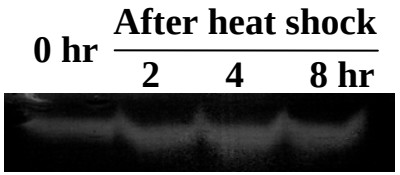

Supplemental figure 4. FOXO3a degrades fibronectin, leading to inhibition of cell-ECM interaction.

A. Immunofluorescent microscopy of fibronectin.

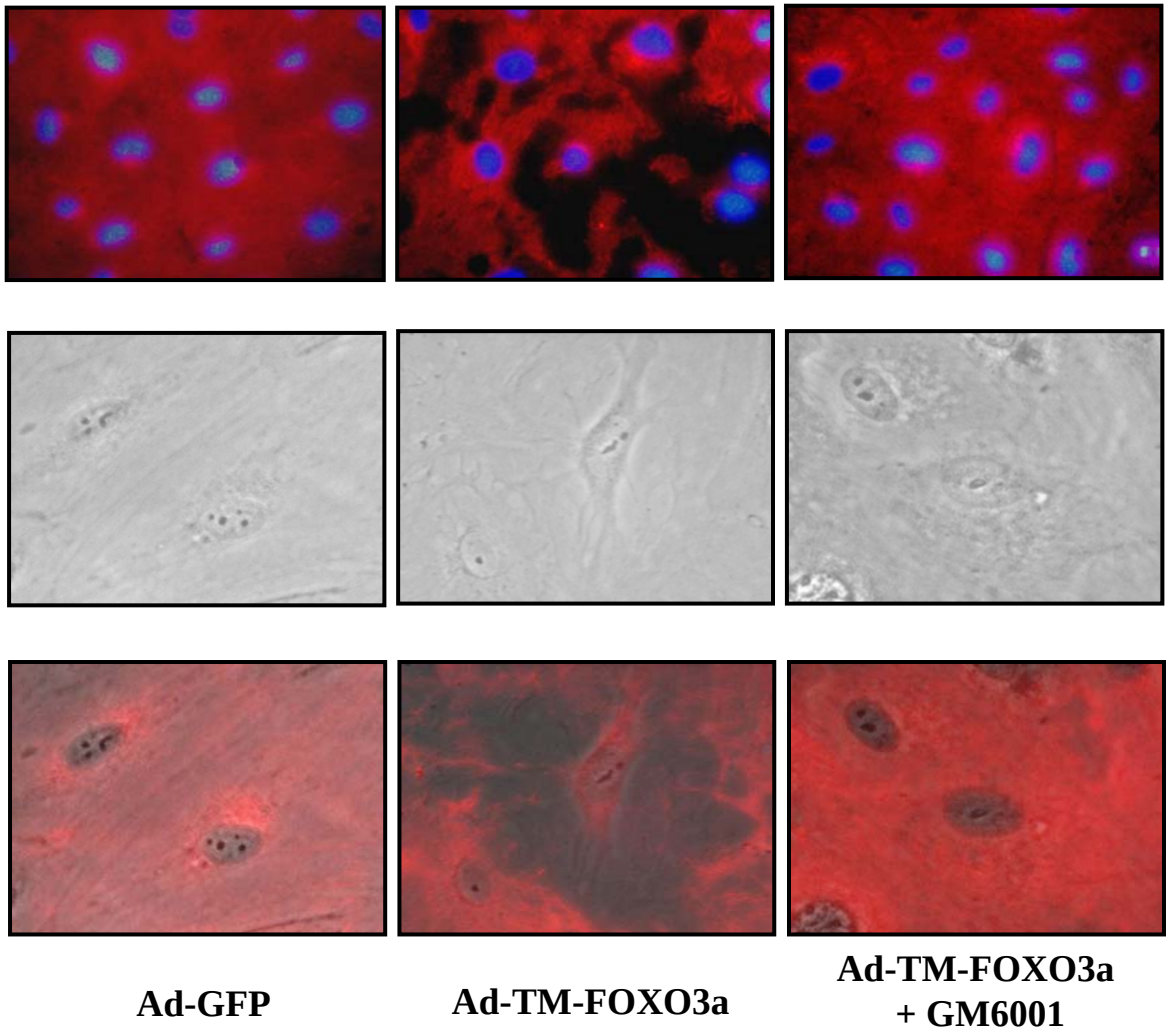

Ad-GFP | Ad-TM-FOXO3a | Ad-TM-FOXO3a + GM6001

B. Fibronectin degradation assay.

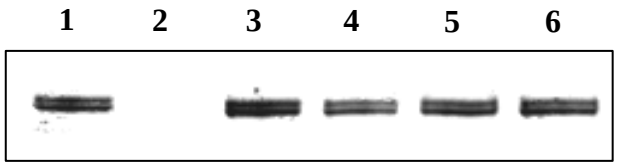

1. Only Fibronectin,
2. Only supernatant
3. Ad-GFP, 4. Ad-TM-FOXO3a
5. Ad-TM-FOXO3a + GM6001 (5μM)
6. Ad-TM-FOXO3a + GM6001 (10μM)

C. Adhesion assay.

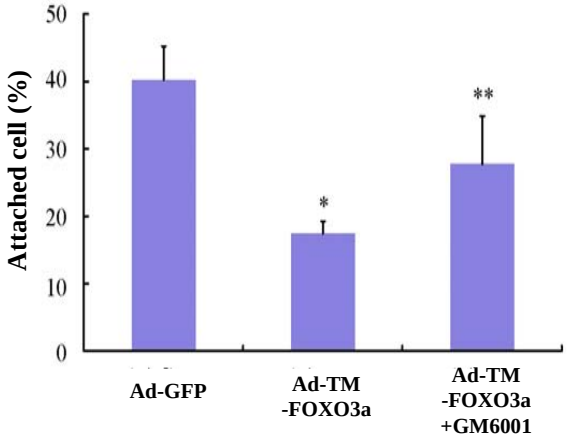

Supplemental figure 5. Figures supplementing ‘Supplemental figure 4B’ regarding fibronectin degradation

A. Another ELISA to supplement Figure 4B

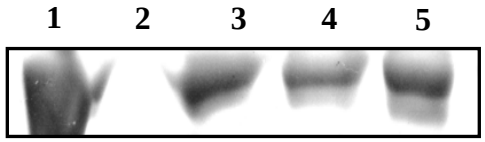

1. Only Fibronectin,
2. Only supernatant
3. Ad-GFP, 4. Ad-TM-FOXO3a
5. Ad-TM-FOXO3a + GM6001 (10μM)

B. TINA densitometry to supplement Figure 4B

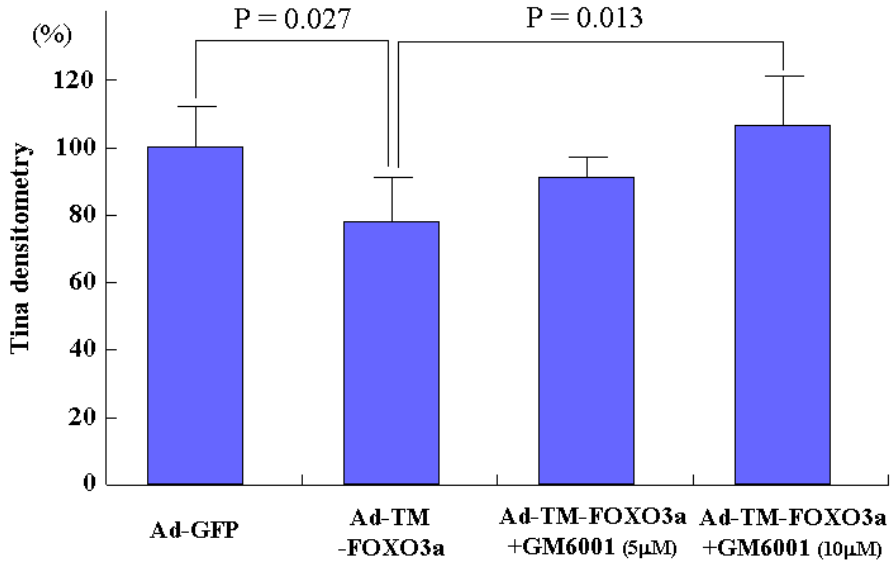

Supplemental figure 6. Morphological and functional evaluation of endothelial denudation

A. Macroscopic photographs of the luminal surface of harvested arterial segments with Evans blue stain

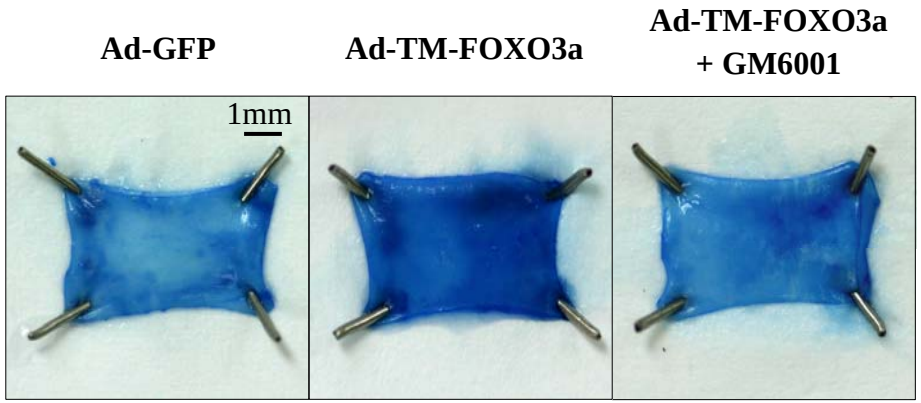

B. Densitometry for unstained area

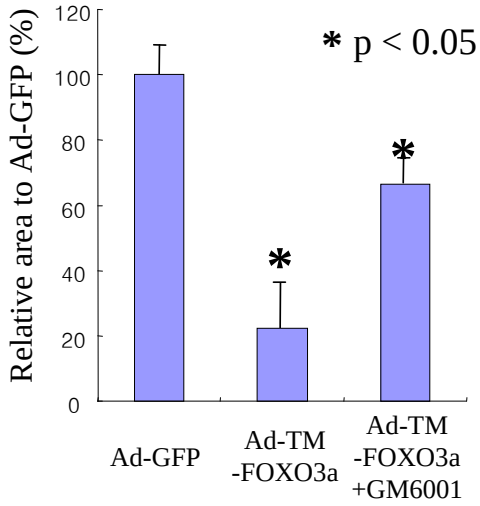

C. Morphometry of Figure 5A

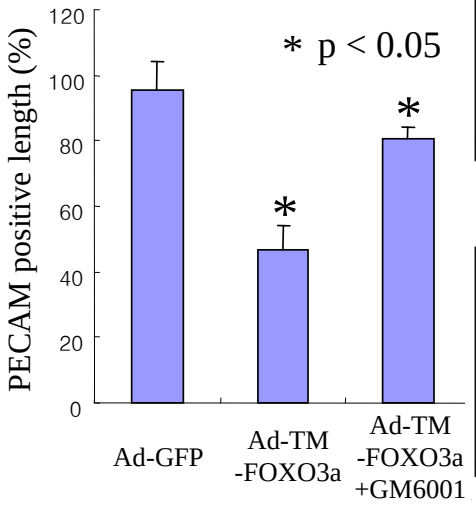

D. Representative figures among triplicated organ chamber experiments of harvested blood vessels transfected with the indicated adenovirus.

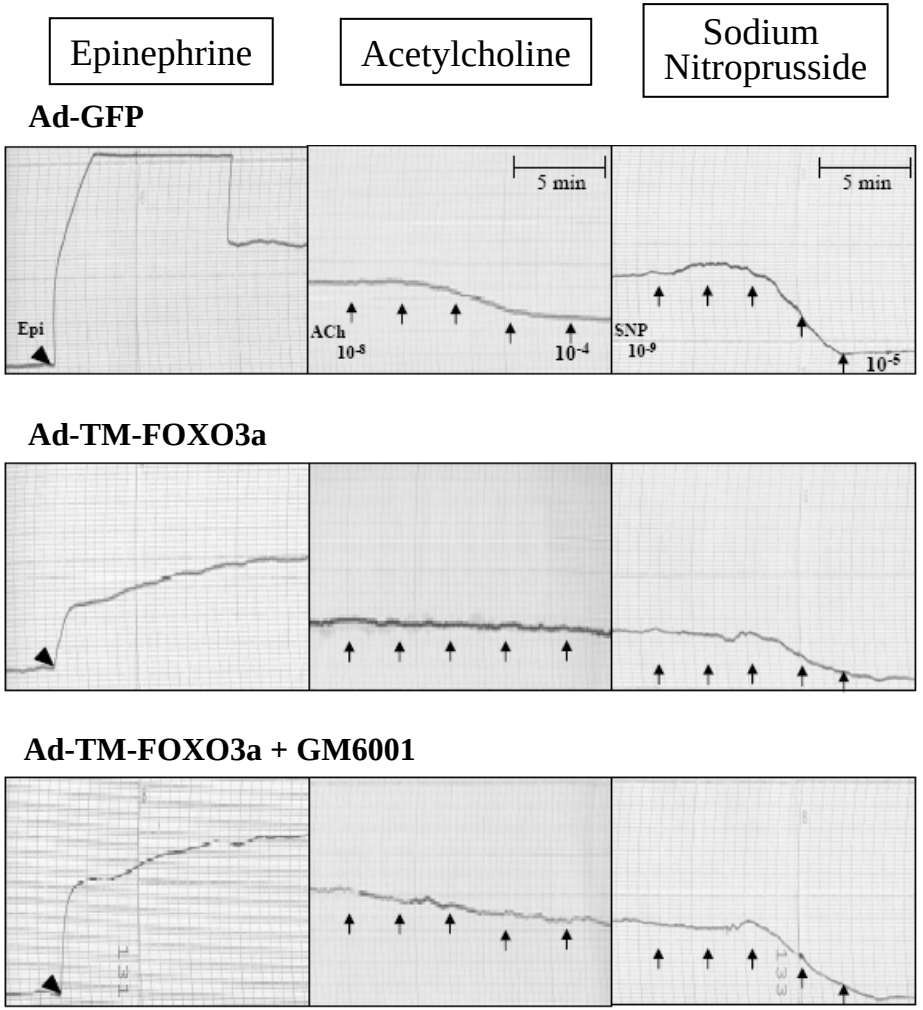

Legends for supplemental figures.

Supplemental figure 1. Validation of adenoviral vectors

For gene transduction, cells were transfected with 25MOI of the adenoviral vector. With this dose, we confirmed the transfection efficacy was more than 90% at 24 hours. As each adenoviral vector also contained GFP sequence, transfection efficacy can be confirmed by visualization of the green fluorescence (GFP) of transduced cell.

(A) Immunoblot analysis of HUVEC transfected by either Ad-GFP, Ad-WT-FOXO3a, or Ad-TM-FOXO3a for phosphor-FOXO3a, total FOXO3a, and α-tubulin. Ad-TM(triple mutant)-FOXO3a was constructed by replacing three phosphorylation sites, Thr32, Ser253, and Ser315 with alanine residues, thus unphosphorylatable by Akt and constitutively active. Bands of total FOXO3a are clear and even in both groups of HUVEC transfected with Ad-WT-FOXO3a and Ad-TM-FOXO3a, suggesting well-controlled and similar transfection rates among HUVECs. Under the same transfection rates, phosphor-FOXO3a was well detected in Ad-WT-FOXO3a, whereas it was negligible in Ad-TM-FOXO3a, suggesting that WT is phosphorylatable and TM is not. Endogenous FOXO3a expression was observable in Ad-GFP lane when the blot was exposed longer. (B) Immunoblot analysis for phosphorylated form and total FOXO3a in

HUVECs transfected with three different adenoviral constructs of FOXO3a; WT [wild type], TM [triple mutant, unphosphorylatable], and DN [dominant negative, truncated at C-terminal transactivation domain]. Phosphorylated FOXO3a was observed in WT-FOXO3a lane. The size of DN-FOXO3a is shorter than that of WT- or TM-FOXO3a. Endogenous FOXO3a expression was observable in Ad-GFP lane when the blot was exposed longer. (C) Differences in cytotoxicity on HUVEC between three adenoviral constructs of FOXO3a in the presence of 10% FBS. Cytotoxicity was greatest in HUVEC infected with Ad-TM-FOXO3a, least with Ad-DN-FOXO3a. (D) Differences in pro-apoptotic action on HUVEC between adenoviral constructs of FOXO3a in the absence of FBS. Serum deprivation-induced apoptosis was greatest in Ad-TM-FOXO3a and Ad-WT-FOXO3a, whereas least in Ad-DN-FOXO3a. Note that the difference between TM and WT becomes greater in the presence of serum than in the absence of serum, because WT-FOXO3a can be phosphorylated and inactivated in the presence of serum, but TM-FOXO3a is not.

Supplemental figure 2. MMP-3 specific knock-down experiments using MMP-3 siRNA

(A) RT-PCR of MMP-3 16 hours after transfection with the indicated adenovirus.

Control siRNA or MMP-3 siRNA were treated 24 hours prior to the indicated adenovirus instillation. MMP-3 mRNA expression was increased after transfection of Ad-TM-FOXO3a, which was completely blocked by MMP-3 siRNA. (-) : no RNA loaded negative control (B) Casein and gelatin zymography. In casein zymography (upper panel), major bands of 57 kDa due to the protease activity of MMP-3 were clearly observed. MMP-3 enzymatic activity was clearly shown to be increased after transfection of Ad-TM-FOXO3a, but the increment was completely reversed by MMP-3 siRNA. Similarly, the increased gelatinolytic activity of MMP-2 (72kDa) following transfection of Ad-TM-FOXO3a was also found reversed with MMP-3 siRNA. (C) Morphologic change of HUVECs 16 hours after transfection of the indicated adenovirus ± siRNA. Plain (upper panels) and fluorescent (lower panels) microscopic findings of HUVECs 16 hours after transfection with 25 MOI of the indicated adenoviral vectors and the indicated siRNA. TM-FOXO3a gene trnasduction induced significant cytotoxicity of HUVEC, which was significantly reversed by MMP-3 siRNA. Magnification x 200. (D) FACS analysis for hypodiploid DNA indicating apoptotic cells. TM-FOXO3a gene transfer induced significant apoptosis of HUVEC, which was significantly reversed by MMP-3 siRNA.

Supplemental figure 3. Activation of endogenous FOXO3a and MMPs in ECs under stressful conditions.

(A) Serial immunoblot analysis of endogenous FOXO3a in nuclear fraction and in cytosolic fraction from 0 to 24 hours after serum starvation without adenoviral transfection. Serum starvation increased nuclear FOXO3a from 6 hours, suggesting that stressful condition may activate FOXO3a in ECs. CREB (cyclic-AMP response element binding protein) indicates nuclear fraction. (B) Casein and gelatin zymography. Serum starvation stimulated the activities of MMP-3 and then MMP-2 time-dependently in ECs. (C) Immunofluorescent staining for endogenous FOXO3a after heat incubation (42ºC). In normal culture condition of ECs without heat shock, the endogenous FOXO3a located in cytoplasm, thus remaining inactive (Upper left). Heat shock rapidly translocated endogenous FOXO3a into nucleus, indicating activation of endogenous FOXO3a (Lower left). As a positive control for nuclear localization of FOXO3a, Ad-TM-FOXO3a-transfected ECs are shown in the upper right panel. Magnification x 200. (D) Immunoblot analysis of FOXO3a in nuclear and cytosolic fraction after heat shock. Heat shock treatment induced nuclear translocation of endogenous FOXO3a in ECs. (E) Casein zymography for MMP-3. Heat shock treatment induced MMP-3 activity over time. (F) Bar graph illustrates the decreased cell viability after heat shock, which was

partially reversed by MMP inhibitor or DN-FOXO3a transfection. Data are expressed as mean ± SE (* P<0.01, n = 6).

Figure 4. FOXO3a degrades fibronectin, leading to inhibition of cell-ECM interaction.

(A) Immunofluorescent microscopy of fibronectin. HUVECs were transfected with Ad-GFP (left), Ad-TM-FOXO3a (middle), or Ad-TM-FOXO3a in the presence of GM6001 (right). (Magnification x 200). Bright field microscopic findings of HUVECs on fibronectin-coated dishes were on second rows. Middle and lower panels showed merged images with a fibronectin immunofluorescent image (magnification x 600). (B) Fibronectin degradation assay. (C) Adhesion assay. Media containing adenoviral vectors (25 MOI) were added to HUVEC ($1x10^4$cells/well) seeded on the fibronectin-precoated plates. After incubation for 24 hours, detached cell were removed and residual viable cells quantified by the WST-1 assay. Results are presented as mean ± SE ($p < 0.05$, n = 16).

Supplemental figure 5. Figures supplementing Figure 4B regarding fibronectin degradation

(A) Fibronectin degradation assay. 50μg of supernatant from each culture dish was mixed with 5μg of fibronectin and incubated at 37℃ for 24 hour. The mixture was transferred to SDS-PAGE gel, stained by Coomassie Blue. Supernatant from HUVEC transfected with Ad-TM-FOXO3a showed a significantly greater fibrinolytic activity on fibronectin than that from HUVEC with Ad-GFP. TM-FOXO3a-induced lysis of fibronectin was reversed by MMP inhibitor GM6001. (B) Quantitative data from TINA densitometry of 5 separate ELISA experiments show that the degree of fibronectin degradation was significantly different and that GM6001 significantly reversed FOXO3a-induced fibronectin degradation.

Supplemental figure 6. Morphological and functional evaluation of endothelial denudation

(A) Macroscopic photographs of the luminal surface of the harvested arterial segments with Evans blue stain. Ad-GFP or Ad-TM-FOXO3a was delivered intraluminally in rabbit carotid arteries. Endothelium-denuded area was stained blue with the Evans blue

dye. (B) Densitometry of extent of denudation area, which was calculated as percentage of endothelium remaining area per total area in three different sections. Bar graphs show significant differences between three groups ($P < 0.05$). (C) Morphometric assessment of the ratio of PECAM-1-positive luminal circumference and total in three different sections, showing significant differences between three groups ($P < 0.05$). (D) Representative figures among triplicated organ chamber experiments of harvested blood vessels transfected with control Ad-GFP, Ad-TM-FOXO3a, or Ad-TM-FOXO3a + GM6001. Initial contractile response by epinephrine (Epi) was used to determine tissue viability in each carotid artery ring (left). And endothelium-dependent vasorelaxation to acetylcholine (middle) and endothelium-independent vasorelaxation to sodium nitroprusside (right) were evaluated.